Fermilab Library
0 1160 0052461 5

SSC-SDC-46

SSC-SDC
SOLENOIDAL DETECTOR NOTES

RADIATION LEVELS IN DETECTORS AT THE SSC

Donald E. Groom

June 20, 1990

SSC–SDC–46
Presented to the *Task Force on Radiation Testing at the SSCL*,
SSCL, 5–6 March 1990 Revised 20 June 1990

Radiation Levels in Detectors at the SSC*

Donald E. Groom†

Lawrence Berkeley Laboratory 50-308, Berkeley CA 94720

Estimates of ionizing dose and neutron fluence have been made for typical SSC detector configurations exposed to radiation from p-p collisions. Using a description of "average events" in conjunction with simulations of secondary processes, it is found for calorimetry that the ionizing dose (D) or neutron fluence (ϕ) can be adequately expressed as

$$D \text{ (or } \phi) = \frac{A}{r^2 \sin^{2+\alpha} \theta} .$$

Here A depends on the process and exposure time, α is slightly less than unity, and r is the distance from the interaction point. Under nominal operating conditions, a metallic calorimeter element 2 m from interaction point and 6° from the beam line is subjected to an annual dose of 30 kGy at electromagnetic shower maximum and an annual neutron fluence of $10^{14}\,\mathrm{cm}^{-2}$ at hadronic cascade maximum.

This report includes provisional correction of an error in electromagnetic dose discovered in the Task Force Report.‡

1. Introduction

An SSC Central Design Group task force was formed to assess radiation levels to be expected in SSC detectors. Its findings are available in a thick report[1], and short versions have also been published[2]. Radiation *effects* were addressed by a separate task force[3]. In this report we present a very brief discussion of radiation levels.

2. Assumptions

On the basis of SSC design parameters and extrapolation from S$\bar{p}$pS and Tevatron operating experience, the following assumptions were made:

- The machine luminosity at $\sqrt{s} = 40$ TeV is $\mathcal{L} = 10^{33}$ cm^{-2}s^{-1}, and the p-p inelastic cross section is $\sigma_{\text{inel}} = 100$ mb. This luminosity is effectively achieved for 10^7 s yr^{-1}. The interaction rate is thus 10^8 s^{-1}, or 10^{15} yr^{-1}.

---

* This report is based on a version published in the *Proceedings of the ECFA Conference on Future Accelerators*, Madrid, Spain (Sept. 1989), but differs from it in three important respects: Table 1 in that report was wrong, and has now been corrected, the electromagnetic dose has been corrected (see the footnote below), and a figure showing the neutron flux in the central cavity as a function of the minimum calorimeter angle has been added.

† For the SSC Central Design Group Task Force on Radiation Levels in the SSC Interaction Regions: F. S. Alsmiller, R. G. Alsmiller, Jr., S. Ban, J. E. Brau, K. W. Edwards, A. Fassò, H. Fesefeldt, T. A. Gabriel , M. G. D. Gilchriese (Chairman), D. E. Groom, H. Hirayama, H. Kowalski, H.W. Kraner, N. V. Mokhov, D. R. Nygren, F. E. Paige, J. Ranft, J. S. Russ, H. Schönbacher, T. Stanev, G. R. Stevenson, A. Van Ginneken, E. M. Wang, R. Wigmans, and T. P. Wilcox, Jr.

‡ The maximum dose in the electromagnetic calorimeter due to incident photons from primary π^0 decay, as reported in Ref. 1 and in numerous conference proceedings, was high by a factor of three because of a trivial conversion error in Appendix 7. Corrected results given here. They are thought to be correct for the metallic part of the calorimeter, but to obtain the dose in the active part of the calorimeter they should probably be corrected upward by the stopping power ratio for the two media. For lead/scintillator the ratio is about 1.6.

- All radiation comes from p-p collisions at the interaction point. For the SSC, the nominal luminosity contributes $(300\ \mathrm{hr})^{-1}$ to the reciprocal current lifetime, so p-p collisions contribute as much radiation as dumping one of the beams into the apparatus every 6 days. Moreover, any process of comparable importance would prevent normal operation of the machine.
- The charged particle distribution is (a) flat in pseudorapidity for $|\eta| < 6$ and (b) has a momentum distribution whose perpendicular component is independent of rapidity, or approximately independent of pseudorapidity:

$$\frac{d^2 N_{\mathrm{ch}}}{d\eta dp_\perp} = H\ f(p_\perp) \tag{1}$$

  (where $p_\perp = p \sin\theta$). Integrals involving $f(p_\perp)$ are simplified by replacing $f(p_\perp)$ by $\delta(p_\perp - \langle p_\perp \rangle)$; in the worst case this approximation introduces an 8% error.
- Gamma rays from π^0 decay are as abundant as charged particles. They have approximately the same η distribution, but half the mean momentum.
- The values $H \approx 7.5$ and $\langle p_\perp \rangle \approx 0.6$ GeV/c for $\sqrt{s} = 40$ TeV are obtained by extrapolating experimental results[4, 5], and are in good agreement with results obtained with standard fragmentation models. These values together with Eq. (1) are thought to describe particle production at the SSC within a factor of two or better.

3. Dose from direct particle production

Since $d\eta/d\Omega = (2\pi \sin^2\theta)^{-1}$, it follows from Eq. (1) that the flux of charged particles from the interaction point passing through a normal area da located a distance $r_\perp$ from the beam line is given by

$$\frac{dN_{\mathrm{ch}}}{da} = \frac{1.2 \times 10^8\ \mathrm{s}^{-1}}{r_\perp^2}\ . \tag{2}$$

In a typical organic material, a relativistic charged particle flux of $3 \times 10^9\ \mathrm{cm}^{-2}$ produces an ionizing radiation dose of 1 Gy, where 1 Gy $\equiv$ 1 joule kg^{-1} (= 100 rads). The above result may then be rewritten as

$$\dot{D} = \frac{0.4\ \mathrm{MGy\ yr}^{-1}}{r_\perp^2} \tag{3}$$

for an absorber much thinner than a nuclear interaction length, where $r_\perp$ is in cm.

In the presence of a magnetic field, low-energy particles make multiple passes through a test sample and so contribute to the dose more than once. This increases dose by about a factor of two.

4. Dose and fluence in a calorimeter

In a medium in which cascades can develop, the ionizing dose or neutron flux is at least roughly proportional to the particle energy striking unit area at a distance r from

the interaction point. The charged particle flux is proportional to $(r^2 \sin^2\theta)^{-1}$, and the energy carried by the particles is proportional to $\langle E\rangle \approx p = p_\perp/\sin\theta$. The dose or fluence at cascade maximum is hence proportional to $1/(r^2\sin^3\theta)$. Symbolically, this logic flow is as follows:

$$\left.\begin{array}{l}\left.\begin{array}{l}\dfrac{dN_{\rm ch}}{d\eta} = \text{Const}\\[2ex] \dfrac{d\eta}{d\Omega} = \dfrac{1}{2\pi\sin^2\theta}\end{array}\right\}\dfrac{dN_{\rm ch}}{d\Omega} = \dfrac{\text{Const}}{\sin^2\theta}\\[2ex] E \approx p = \dfrac{p_\perp}{\sin\theta}\end{array}\right\}\dfrac{dE}{d\Omega} = \dfrac{\text{Const}}{\sin^3\theta}\left.\begin{array}{l}\\[2ex] \dfrac{d\Omega}{da} \propto \dfrac{1}{r^2}\end{array}\right\}\begin{array}{l}\text{Neutron fluence}\\ \text{or ionizing dose}\end{array} = \dfrac{K}{r^2\sin^3\theta} \tag{4}$$

This result is incomplete for a number of reasons. In the first place, the constant K must come from Monte Carlo simulations, hopefully supplemented by experimental measurements. Secondly, since showers lengthen with energy the maximum amplitude is not quite proportional to the incident energy density, so that the power of $\sin\theta$ is a little less than three. This is true for both electromagnetic and hadronic cascades. Finally, hadronic activity increases less rapidly than linearly with energy because π^0 production progressively "bleeds off" more and more energy to the electromagnetic channel as the incident energy increases, further reducing the power of $\sin\theta$ for processes such as neutron production. Even in this case, the combined effect is to reduce the exponent to about 2.7, so the above equation still provides guidance. The inverse r^2 dependence remains rigorously true, providing a serious constraint on detector design.

We rewrite the result as

$$\begin{array}{l}\text{Neutron fluence}\\ \text{or ionizing dose}\end{array} = \sigma_{\rm inel}\int \mathcal{L}dt\,\frac{H\,\langle p_\perp\rangle^\alpha}{r^2}\frac{\text{Const.}}{\sin^{2+\alpha}\theta} = \frac{A}{r^2}\cosh^{2+\alpha}\eta \tag{5}$$

where the dependence on some machine-dependent parameters is made explicit. The second form is obtained with the aid of the identity $\cosh\eta = \sin\theta$.

Values of A and α are given in Table 1 for several relevant situations. The constant A includes factors evaluated with cascade simulation programs as well as constants describing particle production at the interaction point. It is felt that each could introduce an error as large as a factor of two in the results.

For calorimeters the maximum neutron flux, ionizing dose from incident photons, and maximum ionizing dose from incident hadrons are shown in Figs. 1 and 2. The curves are calculated using Eq. (5) and the constants in Table 1.

Under all conditions so far studied, the neutron spectrum shows a broad log-normal distribution peaking at just under 1 MeV, as might be expected for neutron boiloff fol-

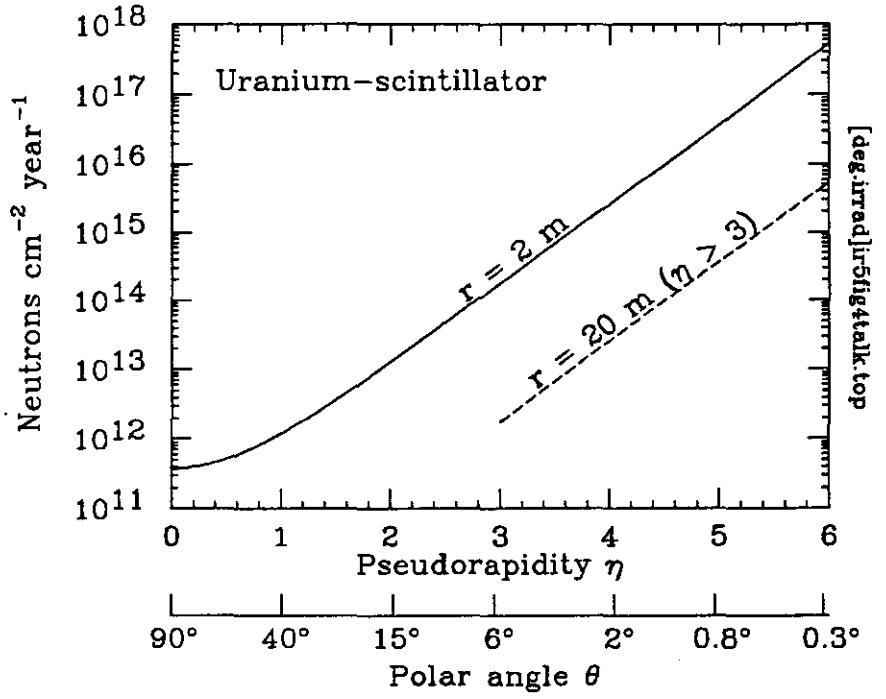

FIG. 1. The maximum neutron flux for a 1:1 uranium:scintillator calorimeter. The solid curve shows the result assuming the maximum occurs at a radius of 200 cm. Also shown is the result for a radius of 20 m, typical of forward detectors, for pseudorapidity > 3.

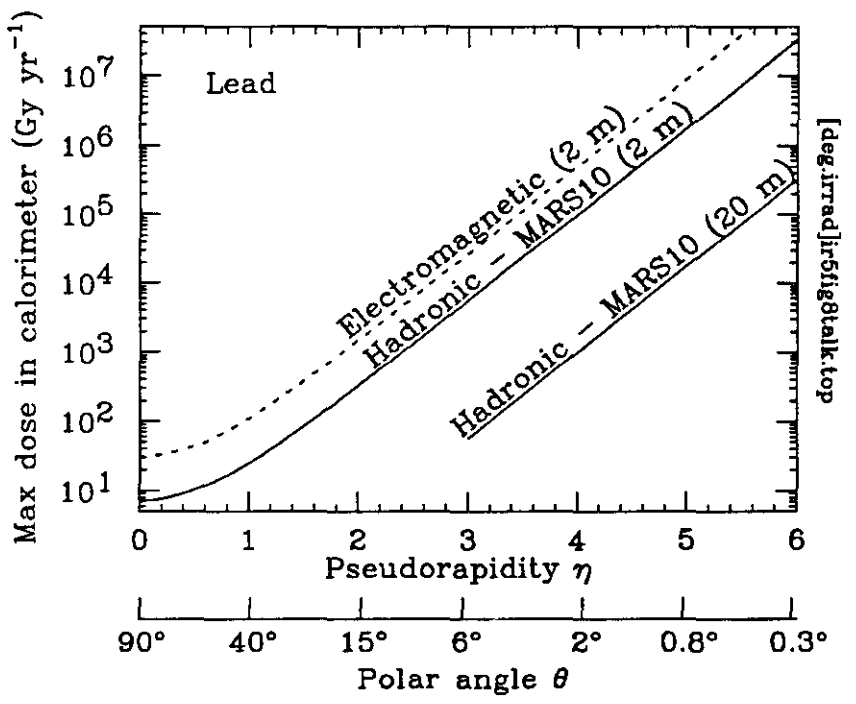

FIG. 2. The maximum hadronic dose as a function of pseudorapidity for a lead sphere, assuming that the maximum dose occurs at the indicated radius. The maximum electromagnetic dose in 1:1 uranium:scintillator is shown by the dashed line. Since the radiation length, nuclear interaction length, and density are nearly identical for the two materials, dose (but not neutron flux) results may be compared directly. The electromagnetic dose has been corrected downward by a factor of three, as described in an earlier footnote. Doses are for the high-Z absorber in the calorimeter, and should probably be corrected upward by a stopping power ratio (1.4 for silicon and 1.6 for scintillator) to obtain the dose in the sensitive material.

lowing nuclear excitation. In the 2 m radius central cavity of a detector with coverage down to $|\eta| = 3$, the average neutron flux is 2×10^{12} cm^{-2}yr^{-1}, including reflection.

Table 1

Coefficients $A/(100\text{ cm})^2$ and α for the evaluation of radiation levels at cascade maximum in SSC calorimetry under nominal operating conditions. At a distance r and angle θ from the interaction point the annual fluence or dose is $A/(r^2 \sin^{2+\alpha}\theta)$.

Quantity	$A/(100\text{ cm})^2$	Units	$\langle p_\perp \rangle$	α
Neutron flux	1.5×10^{12}	cm^{-2}yr^{-1}	0.6 GeV/c	0.67
Dose rate from photons	124*	Gy yr^{-1}	0.3 GeV/c	0.93
Dose rate from hadrons	29	Gy yr^{-1}	0.6 GeV/c	0.89

*Corrected value.

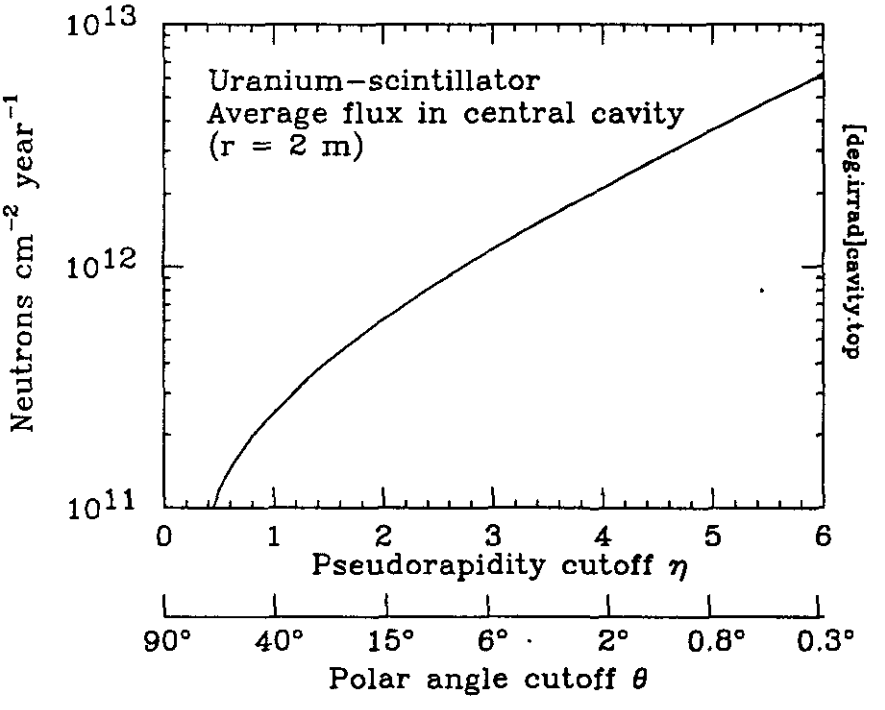

FIG. 3. Average neutron flux in a spherical central cavity with 200 cm radius under nominal SSC operating conditions, in the absence of reflections. Reflections increase the flux by a factor of about two, and the flux scales inversely as the square of characteristic dimensions.

5. Neutrons in the central cavity

Neutrons in the calorimeter may be thought of as a gas in a leaky container. Some (the "albedo neutrons") diffuse back into the central cavity. These have the same "1 MeV" spectrum as do all other neutrons in the environment. Since cascade maxima occur deeper in the calorimeter with increasing energy, the number of albedo neutrons scales only weakly (as about the 0.5 power) with the energy of an incident hadron. The number of neutrons injected per event per pseudorapidity interval is approximately given by

$14.5 \cosh^{0.5} \eta$, as shown in Fig. 5-3 of Ref. 1. The average flux in the cavity is obtained by integrating this function over the region subtended by the central detector. The result is shown in Fig. 3 for a spherical detector with a 200 cm inside radius, in the absence of secondary scattering ("reflection"). Note that most contributions to the integral come from the smallest-angle parts of the calorimeter. Scattering enhances the average flux by a factor of about two, and tends to make it more uniform. With realistic reflection and a cutoff at $|\eta| = 3$, the flux near the ends of the cavity is nearly three times the flux at the center, and the flux near the calorimeter at 90° is about 60% lower than at the center (Wilcox, p. 191 of Ref. 1).

Gabriel and Lillie have investigated the effect of a polyethylene "liner" on the inside surface of the calorimeter[6]. The found that a 10 cm liner reduces the flux in the cavity by an order of magnitude. Matthews has pointed out[7] that most of the reduction can probably be achieved if the hydrogenous layer only covers a small region near the minimum angles, but detailed simulations have yet to be made.

The flux in the cavity scales as the inverse square of the characteristic dimensions, but for a different reason than for the flux in the calorimeter: it is proportional to the average path length of a neutron in the cavity divided by the volume.*

6. Scaling to other machines

Using the scaling discussed in connection with Eq. (5) above, examples of scaling to other accelerators are given in Table 2. It should be noted that the assumption that all radiation comes from the interaction point does not apply to the present generation of accelerators.

Table 2

A rough comparison of beam-collision induced radiation levels in calorimetry at the Tevatron, УНК, high-luminosity LHC, and SSC.

	Tevatron	УНК-3	LHC	SSC
$\sqrt{s}$ (TeV)	1.8	6	16	40
$\mathcal{L}_{\rm nom}$ (cm^{-2}s^{-1})	2×10^{30}	4×10^{32}	$4 \times 10^{34\dagger}$	1×10^{33}
$\sigma_{\rm inel}$	59 mb	80 mb	86 mb	100 mb
H	4.1	4.5	6.3	7.5
$\langle p_\perp \rangle$ (GeV/c)	0.46	0.52	0.55	0.60
Scale factor‡	5×10^{-4}	0.2	27	1

† High-luminosity option.

‡ Proportional to $\mathcal{L}_{\rm nom}\, \sigma_{\rm inel}\, H\, \langle p_\perp \rangle^{0.7}$

* In the approximation of constant flux, this path length may be replaced by the mean chord. For a solid whose surface everywhere has curvature with the same sign, the mean chord is equal to four times the volume divided by the surface area[8].

7. References

1. "Report of the Task Force on Radiation Levels in the SSC Interaction Regions," ed. by D. E. Groom, SSC Central Design Group Report SSC-SR-1033 (June 1988).
2. D. E. Groom, Nucl. Instrum. Methods **A279**, 1 (1989);
   D. E. Groom, pp. 711–716 in *Proc. of the 1988 Summer Study on High Energy Physics in the 1990's*, Snowmass CO, June 27–July 15, 1988, ed. S. Jensen, World Scientific (1989);
   D. E. Groom, *Proc. of the Workshop on Calorimetry for the Superconducting Super Collider*, Tuscaloosa, Alabama, 13–17 March 1989, ed. by R. Donaldson and M. G. D. Gilchriese, World Scientific (to be published, June 1990).
3. "Radiation Effects at the SSC," ed. by M. G. D. Gilchriese, SSC Central Design Group Report SSC-SR-1035 (June 1988).
4. F. Abe *et al.* (CDF), Phys. Rev. Lett. **61**, 1819 (1988).
5. G. J. Alner *et al.* (UA5), Z. Phys. C **33**, 1-6 (1986).
6. T. A. Gabriel and R. A. Lillie, SSC Central Design Group Note SSC-N-545 (1988).
7. J. A. J. Matthews, private communication (1990).
8. A. Cauchy, "Memoire sur la rectification des courbes et la quadrature des surfaces courbes" (1850); reprinted in *Ouvres Completes*, Vol. 2, Gauthier Villard, Paris (1908);
   E. Czuber, "Zur Theorie der geometrischen Wahrscheinlichkeiten," Sitzungsber. Akad. Wiss. Wien Abt. 2, 90, 719-742 (1884).